

Dynamic changes of canopy-scale mesophyll conductance to CO₂ diffusion of sunflower as affected by CO₂ concentration and abscisic acid

RUDI SCHÄUFELE¹, JIRI SANTRUCEK^{2,3} & HANS SCHNYDER¹

¹Lehrstuhl für Grünlandlehre, Technische Universität München, Alte Akademie 12, D-85350, Freising-Weihenstephan, Germany and ²Department of Plant Physiology, Faculty of Science, The University of South Bohemia and ³Institute of Plant Molecular Biology, Biology Centre of the Academy of Sciences of the Czech Republic, Branišovská 31, České Budějovice CZ-370-05, Czech Republic

ABSTRACT

Leaf-level measurements have shown that mesophyll conductance (g_m) can vary rapidly in response to CO₂ and other environmental factors, but similar studies at the canopy-scale are missing. Here, we report the effect of short-term variation of CO₂ concentration on canopy-scale g_m and other CO₂ exchange parameters of sunflower (*Helianthus annuus* L.) stands in the presence and absence of abscisic acid (ABA) in their nutrient solution. g_m was estimated from gas exchange and on-line carbon isotope discrimination (Δ_{obs}) in a ¹³CO₂/¹²CO₂ gas exchange mesocosm. The isotopic contribution of (photo)respiration to stand-scale Δ_{obs} was determined with the experimental approach of Tcherkez *et al.* Without ABA, short-term exposures to different CO₂ concentrations (C_a 100 to 900 $\mu\text{mol mol}^{-1}$) had little effect on canopy-scale g_m . But, addition of ABA strongly altered the CO₂-response: g_m was high (approx. 0.5 mol CO₂ m⁻² s⁻¹) at $C_a < 200 \mu\text{mol mol}^{-1}$ and decreased to <0.1 mol CO₂ m⁻² s⁻¹ at $C_a > 400 \mu\text{mol mol}^{-1}$. In the absence of ABA, the contribution of (photo)respiration to stand-scale Δ_{obs} was high at low C_a (7.2‰) and decreased to <2‰ at $C_a > 400 \mu\text{mol mol}^{-1}$. Treatment with ABA halved this effect at all C_a .

Key-words: *Helianthus annuus*; canopy CO₂ exchange; mesocosm; mesophyll and stomatal conductance; photosynthesis; photosynthetic and (photo)respiratory ¹³C discrimination; respiration.

INTRODUCTION

Mesophyll conductance (g_m) limits the diffusive flux of CO₂ from the substomatal air space to the sites of carboxylations (Lloyd *et al.* 1992; Epron *et al.* 1995; Evans & von Caemmerer 1996; Flexas *et al.* 2008). This limitation is complex, as it involves diffusion through intercellular airspaces and in the liquid phase through cell wall, plasma membrane and cytosol, and the envelope and stroma of the chloroplast (Evans *et al.* 2009). Recent research has revealed strong

short-term, reversible and acclimation responses of g_m to several environmental factors, such as light, temperature, drought, salinity and CO₂ (see Flexas *et al.* 2008 for a compilation of g_m responses). This reversible or adaptive component appears to be associated with the conductance of membranes, which may be modified by the expression of cooporins (Hanba *et al.* 2004; Flexas *et al.* 2007), which are aquaporins capable of transporting CO₂ across plasma membranes (Terashima *et al.* 2006).

Interestingly, adaptive responses of g_m to single environmental drivers do not always agree in direction and magnitude in different experiments with different species. In most cases, g_m increases with decreasing atmospheric CO₂ (e.g. Flexas *et al.* 2007). However, g_m did not respond to CO₂ in *Triticum aestivum* (Tazoe *et al.* 2009) and *Raphanus sativus* (von Caemmerer & Evans 1991). Finally, also a biphasic response of g_m has been found in *Helianthus annuus* (Vrabel *et al.* 2009) with g_m increasing with increasing CO₂ below 200 $\mu\text{mol mol}^{-1}$ and decreasing when CO₂ was increased beyond.

The negative g_m response to water stress and salinity is fairly consistent among species (see compilation of Flexas *et al.* 2008). Also, the majority of studies agree that g_m decreases with leaf age, decreasing nitrogen content and shading. However, these factors often co-vary, making it difficult to unravel the underlying mechanism. Piel *et al.* (2002) showed a marked difference in g_m between sun and shade leaves of *Juglans* sp., but these leaves also differed in nitrogen content. A similar co-variation was observed by Niinemets *et al.* (2005) in Mediterranean evergreen species, where the decreasing nitrogen content with leaf age was accompanied by decreasing g_m . In herbaceous plants older leaves become successively more shaded during canopy development when nitrogen is re-allocated to younger leaves formed near the top of the canopy (Connor, Sadras & Hall 1995). Both factors may affect g_m .

The g_m response to a particular environmental driver – for example, CO₂ – may well depend on interactions with other factors. However, such studies are rare. No interaction between irradiance and CO₂ was observed as either both parameters did not affect g_m (*Triticum aestivum*; Tazoe *et al.* 2009) or lowering irradiance decreased g_m but had no effect

Correspondence: R. Schäufele. e-mail: schaeufele@wzw.tum.de

on the general response to CO₂ (*Banksia* species; Hassiotou *et al.* 2009). When studying the interaction of CO₂ and drought on g_m , care must be taken for co-varying parameters as explained earlier. Drought induced changes in relative water content might affect g_m via anatomical or morphological changes without altering the physiology. In this respect, exogenous application of abscisic acid (ABA) is a useful tool to mimic drought effects on stomatal conductance without affecting the morphology of leaves.

Thus, in this work, we addressed the following main questions: (1) does canopy-scale g_m respond dynamically to short-term variation of CO₂ similar to the response of leaves? and (2) does ABA influence the g_m response to CO₂?

To this end, we used a mesocosm-scale ¹³CO₂/¹²CO₂ gas exchange method (Schnyder *et al.* 2003) and we estimated g_m using the carbon isotope-based approach of Evans *et al.* (1986), Evans & von Caemmerer (1996) and Flexas *et al.* (2007), as modified for canopy-scale measurements according to Tcherkez *et al.* (2010). Finally, we minimized isotopic non-steady states (which can cause artefacts in the determination of g_m ; Tazoe *et al.* 2009) by growing plants and performing all ¹³CO₂/¹²CO₂ exchange measurements in the same isotopic environment.

MATERIALS AND METHODS

Plant material and growth conditions

Plants of sunflower (*Helianthus annuus* L., cv. Optisol, CARG, BSA-Nr. 241) were sown individually in plastic pots (35 cm deep, 5 cm diameter), filled with 0.8 kg of washed quartz sand (0.4–0.8 mm particle size), transferred to four growth cabinets (Conviron E15, Conviron, Winnipeg, Canada) and arranged at a density of 78 plants m⁻². Throughout the experiment an automatic drip irrigation system supplied nutrient solution [modified half-strength Hoagland solution with 7.5 mM N L⁻¹; composition: 2.5 mM KNO₃, 2.5 mM Ca(NO₃)₂, 1 mM MgSO₄, 0.5 mM KH₂PO₄, 0.1 mM Fe-ethylenediaminetetraacetic acid (EDTA), 23 μM H₃BO₃, 4.6 μM MnCl₂, 0.4 μM ZnSO₄, 0.16 μM CuSO₄, 0.26 μM H₂Mo₈O₄] to every pot every 4 h. The supply rate was adjusted weekly to satisfy the water demand of plants. Light was supplied by cool white fluorescent tubes and incandescent lamps. Irradiance at the top of each canopy was maintained at 600 μmol m⁻² s⁻¹ photosynthetic photon flux density (PPFD) during the 16 h photoperiod. Temperature was controlled at 20/16 °C and relative humidity at 75/85% during the light and dark periods of the day. At 28 d after sowing ABA (Sigma-Aldrich, Seelze, Germany) dissolved in methanol was added to the nutrient solution of two growth cabinets. The final ABA concentration in the nutrient solution was 20 μM L⁻¹.

Gas exchange measurements and isotope analysis

The four growth cabinets formed part of the ¹³CO₂/¹²CO₂ gas exchange and labeling system described by Schnyder

et al. (2003). In short, air supply to the growth cabinets was generated by mixing CO₂- and H₂O-free air with CO₂ of known carbon isotope composition ($\delta^{13}\text{C}$, where $\delta^{13}\text{C} = [(R_{\text{sample}}/R_{\text{standard}}) - 1]$, and R the ¹³C/¹²C ratio in the sample or Vienna Pee Dee belemnite (VPDB) standard. The CO₂-free dry air was produced by passing compressed ambient air through an absorption dryer (KEN 3100, Zander, Essen, Germany) filled with a molecular sieve (activated aluminium oxide F200, Alcoa, Houston, TX, USA). The dryer was fed by a screw compressor (S40, Boge, Bielefeld, Germany), which compressed ambient air to ~0.7 MPa at a rate of ≤300 m³ h⁻¹. After passage through the dryer, the air had a residual CO₂ concentration of <0.5 μmol mol⁻¹ and its dew point was ≤70 °C. The rate of air supply and the CO₂ concentration in air injected into the growth cabinets was controlled by four independently operated gas mixing systems. Each served one cabinet and comprised two computer-operated mass-flow controllers (FC-2925V for air and FC-2900 4S for CO₂, Tylan General, San Diego, CA, USA). A computer-controlled gas sampling system (DMP, Hegnau-Volketswil, Switzerland) sequentially sampled air entering and leaving each growth cabinet. Each air sample was split: CO₂- and H₂O-concentration was analysed with an IRGA (Licor 6262, Li-Cor, Lincoln, NE, USA) and the $\delta^{13}\text{C}$ of CO₂ by an online gas isotope ratio mass spectrometer (IRMS, Delta plus, Finnigan MAT, Bremen, Germany). Air for mass spectrometric analysis was pumped continuously *via* a steel capillary from the gas sampling system to a 300 μL sample loop which was attached to a six-port Valco valve (Valco Instruments Co. Inc., Houston, TX, USA) mounted in a GC interface (GP-GC Interface, Finnigan MAT, Bremen, Germany). Air samples were fed to the mass spectrometer by periodically flushing the sample loop with He carrier gas and flushing the content through a Nafion® water trap and a GC column (25 m × 0.32 mm Poraplot Q, Chrompack, Middelburg, Netherlands). Then, the CO₂ was introduced into the ion source of the IRMS via a glass capillary (0.1 mm i.d.) connected to the interface via an open split.

The system allowed a high frequency of sampling (approx. one sample per 2 min), so that each inlet and outlet of the four growth cabinets was sampled every 25 min. Each sample was compared with a VPDB-gauged working standard reference CO₂ gas. The external precision (standard deviation) at 300 μmol mol⁻¹ CO₂ was <0.2‰ for $\delta^{13}\text{C}$.

During the entire experiment, including the establishment phase of the stands, two of the growth cabinets were supplied with CO₂ from a fossil-organic source ($\delta^{13}\text{C}$ -47.1‰) and two with CO₂ from a mineral source ($\delta^{13}\text{C}$ -5.4‰; both CO₂: Messer Griesheim, Frankfurt a.M., Germany).

Rates of net CO₂ exchange in light (A , μmol CO₂ m⁻² s⁻¹) were calculated as the difference between the CO₂ fluxes entering (F_{in} , μmol CO₂ s⁻¹) and leaving (F_{out} , μmol CO₂ s⁻¹) the cabinets divided by the cabinets' ground area (s , 1.4 m²):

$$A = (F_{\text{in}} - F_{\text{out}}) / s. \quad (1)$$

δ_A , the $\delta^{13}\text{C}$ of net CO_2 exchange of canopies during the light was obtained by isotopic mass balance:

$$\delta_A = (\delta_{\text{in}}F_{\text{in}} - \delta_{\text{out}}F_{\text{out}})/(F_{\text{in}} - F_{\text{out}}) \quad (2)$$

with subscript *in* and *out* denoting the inlet and outlet of the growth cabinet. δ_{Rn} , the $\delta^{13}\text{C}$ of CO_2 respired in the dark was obtained in the same way using measurements taken during the dark period.

On-line ^{13}C discrimination (Δ_{obs}) was calculated according to Evans *et al.* (1986):

$$\Delta_{\text{obs}} = \frac{\xi(\delta_{\text{out}} - \delta_{\text{in}})}{1 + \delta_{\text{out}} - \xi(\delta_{\text{out}} - \delta_{\text{in}})} \times 10^3, \quad (3)$$

with $\xi = \frac{C_{\text{in}}}{C_{\text{in}} - C_{\text{out}}}$ and C the CO_2 concentration at standard humidity.

C_{out} was maintained at $310 \mu\text{mol mol}^{-1}$ (SE = $0.6 \mu\text{mol mol}^{-1}$) throughout the experiment. C_{in} and the flux of air into the chamber were adjusted at intervals of 2 to 3 d to maintain ξ between 5 and 8. Thus, with constant Δ_{obs} during canopy development, $\delta^{13}\text{C}$ of the CO_2 in the cabinet atmosphere (δ_{out}) was constant (SE = 0.04‰ for both CO_2) throughout the experiment.

Transpiration rate (E , $\text{mmol H}_2\text{O m}^{-2} \text{s}^{-1}$) was calculated analogous to A (Eqn 1). Thus, $E = (F_{\text{H}_2\text{O out}} - F_{\text{H}_2\text{O in}})/s$, with *out* designating the flux of water vapour leaving the cabinet ($\text{mmol H}_2\text{O s}^{-1}$) and *in* that added to cabinet air by the individual cabinets' humidification system (note that air entering the chambers was dry; see earlier discussion). The humidification system controlled the water vapour concentration in cabinet air by adding just enough vapour to match the difference between that generated by E and the nominal water vapour concentration of the chamber. Water addition by the humidification system occurred by activation (opening) of spray nozzles whenever the measured vapour concentration decreased below the nominal concentration. The rate of vapour addition of each sprayer was obtained from a calibration of vapour production versus nozzle activation times. E was recorded for each step during CO_2 response measurements for approximately 15 min when the CO_2 concentration at the chamber outlet had reached the new steady state. Evaporation from the sand surface (15% of chamber area) was a negligible component of (evapo)transpiration of the closed sunflower canopy. This was true, except for a small evaporation signal during a short period during and after irrigation events when the sand surface of pots was wetted and the relative humidity of chamber increased briefly. Therefore, data were not taken for a period of 20 min after irrigation. The CO_2 response of A and E was measured in duplicate in two growth cabinets.

Calculation of g_m

According to Fick's first law, g_m is expressed as,

$$g_m = \frac{A}{C_i - C_c}, \quad (4)$$

with A the net photosynthesis rate of the stand and C_i and C_c the CO_2 concentrations in the intercellular airspace and in the chloroplast. Canopy-scale on-line carbon isotope discrimination (Δ_{obs}) is (Tcherkez *et al.* 2010):

$$\Delta_{\text{obs}} = a_b \frac{C_a - C_s}{C_a} + a \frac{C_s - C_i}{C_a} + a_m \frac{C_i - C_c}{C_a} + b \frac{C_c}{C_a} - \frac{d^*}{C_a}, \quad (5a)$$

where

$$d^* = eR_d/k + e_h R_h C_a / A + f\Gamma^*, \quad (5b)$$

with C_a and C_s denoting the CO_2 concentration in the atmosphere and at the leaf surface, a_b the fractionation during diffusion through the leaf boundary layer; a that during diffusion in air, a_m the combined fractionation during dissolution of CO_2 in water and fractionation during diffusion of dissolved CO_2 in water; b the fractionation associated with carboxylations, R_d the rate of leaf dark respiration in light; R_h the dark respiration of heterotrophic plant parts (root and stem), k the carboxylation efficiency, Γ^* the CO_2 compensation point in the absence of dark respiration, f the fractionation associated with photorespiration, e the fractionation associated with leaf dark respiration in light and e_h the fractionation associated with respiration of heterotrophic plant parts. d^*/C_a , the last term on the right-hand side of Eqn 5a, represents the effect of total mesocosm respiration in light on Δ_{obs} . This includes photorespiration and daytime dark respiration of autotrophic (leaf) and heterotrophic plant parts and soil, and was termed (photo)respiration (in accordance with Tcherkez *et al.* 2010). This term is a potentially large component of Δ_{obs} as respiration is a much bigger fraction of net CO_2 exchange at mesocosm than at leaf scale, and carbon isotope fractionation in photorespiration and dark respiration of different plant parts is significant (Ghashghaie *et al.* 2003; Klumpp *et al.* 2005). The contribution of (photo)respiration to Δ , d^*/C_a was obtained as:

$$d^*/C_a = \Gamma(b - \Delta^0)/C_a \quad (6)$$

(cf. Eqn 3 in Tcherkez *et al.* 2010), where Δ^0 denotes Δ at the CO_2 compensation point, Γ , of the mesocosm. Δ^0 was estimated as the intercept of a linear regression of Δ_{obs} versus A ('second method' in Tcherkez *et al.* 2010) using the data obtained during the CO_2 response measurements (as presented in Fig. 2a,c). This method has the advantage, that it does not require assumptions on the rates of (photo)respiration of leaves, and respiration of roots and stems and their specific fractionation factors (see discussion in Tcherkez *et al.* 2010).

Mesophyll conductance was calculated using the difference between Δ_{obs} (Eqn 3) and an estimate of Δ assuming infinite g_m (Δ_i):

$$\Delta_i = a_b \frac{C_a - C_s}{C_a} + a \frac{C_s - C_i}{C_a} + b \frac{C_i}{C_a} - \frac{d^*}{C_a}, \quad (7)$$

with a_b 2.9‰ (Farquhar 1983); a 4.4‰ (Craig 1954); b 28.9‰ (McNevin *et al.* 2006).

Leaf boundary layer conductance used to calculate C_s was not measured but assumed to be $750 \text{ mmol m}^{-2} \text{ s}^{-1}$ for water vapour (within the range found for broad-leaved species in greenhouses; Morrison & Gifford 1984; Aphalo & Jarvis 1993; Gan *et al.* 2002). C_i was calculated from stomatal conductance, which was based on measurements of transpiration (E) and leaf temperature. Leaf temperature was measured using six thermocouples evenly distributed within the top 20 cm of the canopy.

The last term in Eqn 7 [i.e. the (photo)respiratory contribution] is the same as the last term in Eqn 5a. Thus, any difference between Δ_i and Δ_{obs} was caused by the difference between C_i and C_c :

$$\Delta_i - \Delta_{\text{obs}} = (b - a_m) \frac{C_i}{C_a} - (b - a_m) \frac{C_c}{C_a} \quad (8)$$

with a_m 1.8‰ (Vogel, Grootes & Mook 1970; O'Leary 1984).

Equation 8 could be solved for C_c as the only unknown and used to calculate g_m using Eqn 1.

RESULTS

Canopy gas exchange and ^{13}C discrimination under growth conditions

A and Δ_{obs} of sunflower canopies were measured in four different mesocosms under growth conditions. Measurements started after canopy closure when A , and Δ_{obs} were near-constant on a day-by-day basis (Fig. 1 and Table 1). A averaged $15.6 \mu\text{mol CO}_2 \text{ m}^{-2} \text{ s}^{-1}$ in the four chambers and varied little between them (Table 1). Similarly, A was quite stable during the course of individual light periods. In general, it decreased slightly between 1 and 15 h in light (Fig. 1a). Δ_{obs} was high in all growth chambers (average 24.1‰). But it was virtually the same in growth chambers with different $\delta^{13}\text{C}_{\text{CO}_2}$ (Table 1).

Effect of ABA on gas exchange and ^{13}C discrimination under growth conditions

ABA had strong effects on A and Δ_{obs} (Fig. 1). A and Δ_{obs} started to decrease immediately after ABA addition to the nutrient solution (data not shown). The effect of ABA on A and Δ_{obs} saturated after about 2 to 3 d when A and Δ_{obs} stabilized at near-constant values. At that time A was $11.8 \mu\text{mol CO}_2 \text{ m}^{-2} \text{ s}^{-1}$, or 25% less than the rate just prior to ABA addition. Again, there was a slight decrease in A throughout the light period. Δ_{obs} was 17.2‰, i.e. 6.9‰ less than before ABA addition (Table 1).

ABA also strongly affected the relationship between $\delta^{13}\text{C}$ of net CO_2 exchanged (δ_A) and the CO_2 respired in the night (δ_{Rn}) or the (photo)respired CO_2 (δ_{PR}). In control canopies, δ_{Rn} was approximately 5‰ enriched relative to δ_A (Table 2). Conversely, δ_{PR} was depleted by 2.6‰ relative to δ_A . After ABA application, δ_{Rn} was still slightly enriched

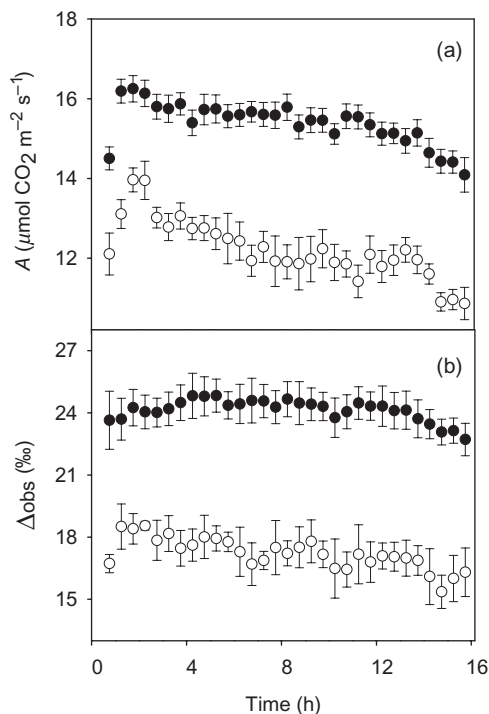


Figure 1. (a) Daytime net CO_2 exchange (A ; $\mu\text{mol CO}_2 \text{ m}^{-2} \text{ s}^{-1}$) and (b) associated on-line carbon isotope discrimination (Δ_{obs}) of sunflower canopies before (full symbols) and after (open symbols) abscisic acid (ABA) addition to the nutrient solution. Data points represent means of half-hourly measurements taken on four (A and Δ_{obs} of control) and two (A and Δ_{obs} of ABA) mesocosms during four (control) and three (ABA) 16 h light periods. SD is indicated by vertical bars.

relative to δ_A (approx. 1‰; Table 2). ABA had a particularly strong effect on δ_{PR} , which was 3‰ enriched relative to δ_A after ABA addition, but was significantly depleted before addition.

Effect of ABA on the CO_2 response of A , Δ_{obs} and transpiration

The CO_2 response of A , Δ_{obs} and canopy conductance was measured on the day before first ABA addition, and after 3 d of ABA addition, when A and Δ_{obs} had decreased to a stable level. All measurements were performed between 2 h of 'lights on' and 6 h before the end of the light period, when A and Δ_{obs} were near constant. In the absence of ABA, A followed the characteristic response of photosynthesis to changes in CO_2 partial pressures (C_a) as described by leaf- or cell-based models of Farquhar, von Caemmerer & Berry (1980) and von Caemmerer and Farquhar (1981) (Fig. 2a). Transpiration also showed a strong response to increasing C_a (Fig. 2b), with the rate decreasing by 30% between 100 and $900 \mu\text{mol mol}^{-1} \text{ CO}_2$. Furthermore, Δ_{obs} increased greatly with increasing C_a (Fig. 2c). At $900 \mu\text{mol CO}_2 \text{ mol}^{-1}$ Δ_{obs} was $28.3\text{‰} [\pm 0.1 \text{ standard deviation (SD)}]$, close to the ^{13}C discrimination value of Rubisco.

Chamber no.	$\delta^{13}\text{CO}_2$ ‰	Before ABA application		After ABA application	
		<i>A</i> $\mu\text{mol CO}_2 \text{ m}^{-2} \text{ s}^{-1}$	Δ_{obs} ‰	<i>A</i> $\mu\text{mol CO}_2 \text{ m}^{-2} \text{ s}^{-1}$	Δ_{obs} ‰
1	-47	16.4	24.3	–	–
2	-47	16.1	24.1	–	–
3	-5	15.3	24.2	12.3	16.9
4	-5	14.5	23.8	11.2	17.5

Table 1. Net mesocosm CO_2 exchange in light (*A*) and associated on-line carbon isotope discrimination (Δ_{obs}) of sunflower stands in four growth chambers (mesocosms)

Growth conditions were identical in the chambers except for the $\delta^{13}\text{C}$ of CO_2 ($\delta^{13}\text{CO}_2$). Data report the mean *A* and Δ_{obs} during 3 d prior to addition of ABA to the nutrient solution, and the mean rate on the third day after abscisic acid (ABA) addition (chambers 3 and 4).

ABA strongly modified the short-term CO_2 responses of *A*, Δ_{obs} and transpiration. ABA had no effect on *A* at $C_a < 150 \mu\text{mol mol}^{-1}$, but at higher C_a *A* was significantly reduced relative to the control (Fig. 2a). At a C_a of $900 \mu\text{mol mol}^{-1}$ *A* was reduced by 25% relative to the control.

Transpiration (*E*) was affected more strongly by ABA addition (Fig. 2b) and the reduction, relative to the control, was similar (near 40%) over the whole range of C_a . Overall, ABA caused a substantial improvement of water use efficiency (*A/E*) at all C_a (Supporting Information Fig. S1). ABA did not affect the sensitivity of *E* to C_a when this sensitivity was expressed as the change in *E* produced by a small change in C_a (dE/dC_a). However, ABA did affect the response of *E* to C_a : an increase from 120 to $860 \mu\text{mol mol}^{-1}$ CO_2 caused a reduction in *E* by 20% in the absence of ABA, while the same change caused a reduction of 40% in the presence of ABA.

ABA and C_a had strong interactive effects on Δ_{obs} . Δ_{obs} was unaffected by ABA when C_a was low. But, the responses of Δ_{obs} to C_a diverged strongly when C_a was increased above $150 \mu\text{mol mol}^{-1}$: Δ_{obs} decreased in the presence of ABA, but increased in its absence. At a C_a of $500 \mu\text{mol mol}^{-1}$, Δ_{obs} was 15‰ in the presence of ABA, 12‰ less than in its absence. In both treatments, changes of C_a above $500 \mu\text{mol mol}^{-1}$ had little effect on Δ_{obs} .

Effect of ABA on the components of Δ_{obs}

Using d^*/C_a (Eqn 6), the (photo)respiratory contribution to Δ_{obs} could be calculated for each measurement taken during the CO_2 response (Fig. 3). This term described the total effect of all respiratory activities of the mesocosm (including photorespiration) on Δ_{obs} measurements in light. In

control canopies (photo)respiratory discrimination was a very significant component of Δ_{obs} at low C_a (7.2‰ at C_a of $120 \mu\text{mol mol}^{-1}$) decreasing strongly with increasing C_a (1‰ at the highest C_a). After ABA application (photo)respiratory discrimination showed a similar shape of the response to a change in C_a . However, at each CO_2 concentration, the contribution to Δ_{obs} was only half of that in control canopies (3.8 and 0.6‰ at the lowest and highest C_a , respectively).

Effect of ABA on the CO_2 response of mesophyll conductance

Canopy-scale mesophyll conductance was calculated from estimates of C_i and C_c , and the net rate of CO_2 fixation (*A*), using Fick's first law (Eqn 1). Estimates of C_i were obtained from *E*, leaf temperature and the vapour pressure deficit of chamber air. Canopy conductance was very high and was ignored in the estimation of C_i . Estimates of C_c were obtained with Eqn 8, using parameters as given in the Materials and Methods section.

In control canopies, the difference $\Delta_i - \Delta_{\text{obs}}$ was highest at low C_a and decreased nearly linearly with increasing CO_2 concentration (Fig. 4a). Again, there was virtually no difference in $\Delta_i - \Delta_{\text{obs}}$ between ABA-treated and control canopies at low C_a . But $\Delta_i - \Delta_{\text{obs}}$ increased with ABA application up to $400 \mu\text{mol mol}^{-1}$ C_a , but did not change with higher CO_2 concentration.

Accordingly, g_m in control canopies averaged $0.45 \text{ mol CO}_2 \text{ m}^{-2} \text{ s}^{-1}$ and hardly responded to C_a (Fig. 4b). In contrast, g_m in ABA-treated canopies strongly responded to C_a : at low C_a , g_m was in the range observed in control canopies, but it decreased exponentially with C_a and attained $<0.1 \text{ mol CO}_2 \text{ m}^{-2} \text{ s}^{-1}$ at the highest CO_2 concentration.

Chamber no.	$\delta^{13}\text{CO}_2$ ‰	Before ABA addition			After ABA addition		
		δ_A	δ_{Rn}	δ_{PR}	δ_A	δ_{Rn}	δ_{PR}
3	-5	-24.4	-19.3	-27.1	-19.6	-18.3	-15.7
4	-5	-25.0	-20.0	-27.6	-19.1	-18.3	-17.0

Table 2. $\delta^{13}\text{C}$ of net CO_2 exchanged in the light (δ_A), $\delta^{13}\text{C}$ of CO_2 respired in the dark (δ_{Rn}) and $\delta^{13}\text{C}$ of (photo)respiratory CO_2 in the light (δ_{PR}) of sunflower canopies grown and measured at $350 \mu\text{mol mol}^{-1}$

Measurements were performed during 3 d prior to addition of abscisic acid (ABA) to the nutrient solution, and on the third day after ABA addition. Data from chambers 3 and 4.

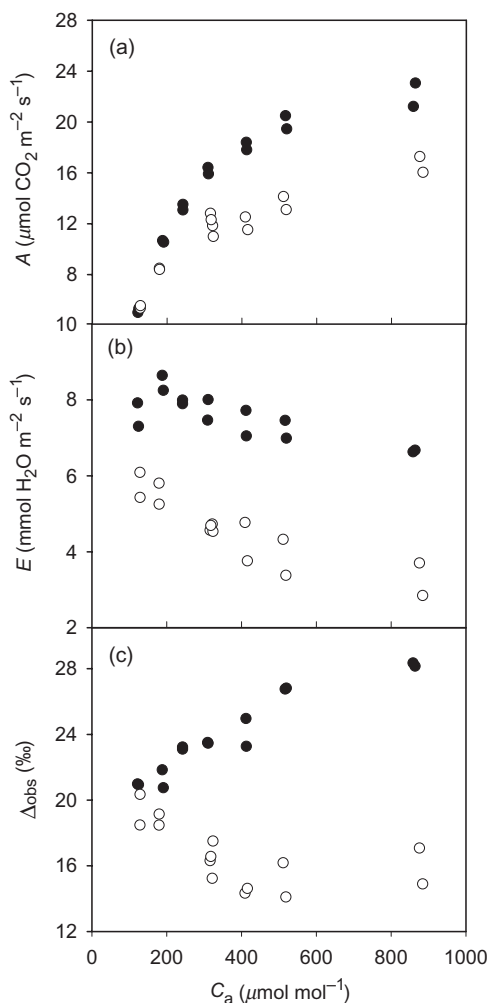


Figure 2. Response of (a) A (b) E and (c) Δ_{obs} of sunflower canopies to a change in C_a , the atmospheric CO_2 concentration. Measurements were performed in the absence (full symbols) and presence (open symbols) of abscisic acid (ABA) in the nutrient solution. Measurements were performed on the day just prior to ABA addition, and on the third day after ABA addition, when A and Δ_{obs} had decreased to a near-constant level. All measurements were performed in two mesocosms. Data points represent single measurements.

Taken together, the CO_2 responses of g_s (not shown, but see Fig. 2b) and g_m implied that the C_c to C_i ratio of ABA-treated canopies decreased with C_a , while it increased in controls (Fig. 5a). In ABA-treated canopies the ratio was ~ 0.8 at a C_a of $<200 \mu\text{mol mol}^{-1}$, decreased to 0.6 up to $400 \mu\text{mol mol}^{-1}$ and remained at ~ 0.6 beyond $400 \mu\text{mol mol}^{-1}$. Conversely, in the control treatment, the ratio increased from ~ 0.8 at a C_a of $<200 \mu\text{mol mol}^{-1}$ to ~ 0.95 at $850 \mu\text{mol mol}^{-1}$. Nevertheless, C_c (and C_i) increased continuously with C_a in both treatments (although to different extents), meaning that the degree of CO_2 limitation of Rubisco decreased with C_a (Fig. 5b,c). Still, because of the very low g_m , C_c barely exceeded $400 \mu\text{mol mol}^{-1}$ at the highest C_a ($870 \mu\text{mol mol}^{-1}$) in the ABA-treated canopies (Fig. 5c).

DISCUSSION

This work revealed a significant co-limitation of canopy photosynthesis by g_m in sunflower under ambient CO_2 . Short-term variation of CO_2 had little effect on g_m in control conditions, but addition of ABA led to dynamic CO_2 -responses of g_m . In the presence of ABA, g_m decreased very strongly and rapidly with increasing CO_2 , significantly decreasing C_c below C_a at ambient to elevated C_a . Decreasing CO_2 to low C_a reversed this effect.

As discussed by Warren (2006), the estimation of g_m with the isotopic method depends on the values of the parameters used for the estimation of Δ_i . These include the rate of (photo)respiration, the fractionation associated with photorespiration and dark respiration in light and the fractionation by carboxylases (cf. Eqn 7), which are all associated with uncertainties. Therefore we elected to use the approach of Tcherkez *et al.* (2010) to estimate discrimination associated with total mesocosm respiration in light (termed '(photo)respiration' and including all photorespiration, and dark respiration by autotrophic and heterotrophic components of the system in the light). This approach avoided assumptions about individual respiratory fractionation factors and rates of photo- and dark respiration in light. The integral contribution of these respiratory activities to mesocosm-scale Δ_{obs} was especially important

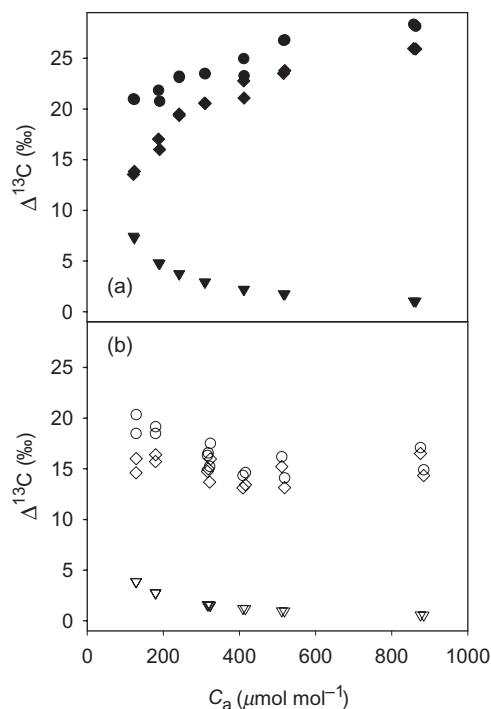


Figure 3. Contribution of photosynthetic (diamonds) and (photo)respiratory carbon isotope discrimination (triangles) to Δ_{obs} (circles) in control (a) and abscisic acid (ABA)-treated (b) sunflower canopies. (Photo)respiratory carbon isotope discrimination corresponds to d^*/C_a (see Eqn 5a,b). Photosynthetic carbon isotope discrimination was obtained as Δ_{obs} minus d^*/C_a . For ease of comparison Δ_{obs} data from Fig. 2c are repeated.

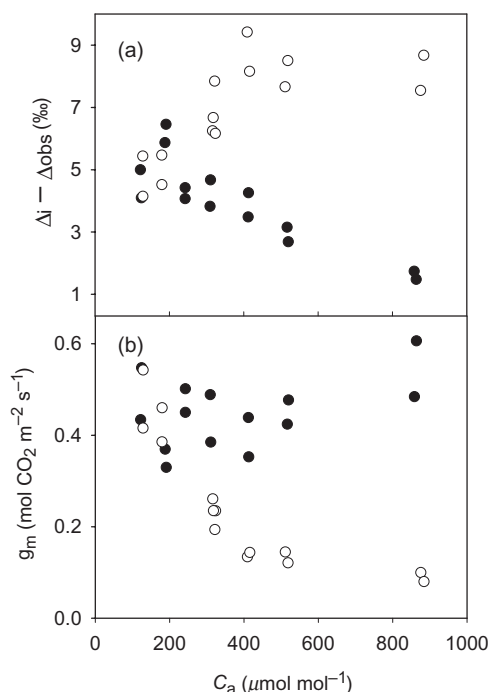


Figure 4. (a) Difference between Δ_i (estimated from gas exchange measurements) and Δ_{obs} (measured by the on-line method) and (b) mesophyll conductance in control (full symbols) and abscisic acid (ABA)-treated (open symbols) sunflower canopies as a function of C_a .

at low C_a , where the (photo)respiratory signal accounted for up to 35 % of Δ_{obs} in the control mesocosm (Fig. 3). This derived from the fact that the ratio of (photo)respiration to gross photosynthesis is highest at low C_a and decreases with increasing C_a .

Importantly, the ranking of the treatments and the shape of the response functions of g_m to C_a were also not altered when we modified the fractionation factors affecting d^* (b and Δ^0 , see Eqn 6) in a wide range. Increasing (decreasing) Δ^0 led to decreasing (increasing) g_m in both treatments without affecting their ranking. In ABA-treated canopies, for example, an increase of Δ^0 from 21.4‰ (i.e. the measured value) to 25‰ caused a decrease in g_m of 13%. Increasing (decreasing) b , led to lower (higher) estimates of g_m in both treatments, again with no effect on treatment ranking. The same was true for the shape of the g_m response to C_a . Also, consideration of canopy-scale heterogeneity in stomatal conductance of leaves (which may vary as a function of leaf position/irradiance, age and ABA effects) would not alter our conclusions. Lloyd *et al.* (1992) have shown that even in situations of very high heterogeneity of stomatal conductance the error in the difference between Δ_i and Δ_{obs} would not exceed 1‰. This error is only a small fraction of the ABA effect on $\Delta_i - \Delta_{\text{obs}}$ observed in our study. Finally, we are very confident that artefacts in Δ_{obs} measurements were insignificant: we observed the same Δ_{obs} for canopies growing in the presence of CO₂ with different $\delta^{13}\text{C}$ (Table 1), meaning that there were no leaks in the

chambers, which could have influenced mesocosm $^{13}\text{CO}_2/^{12}\text{CO}_2$ exchange and, hence, Δ_{obs} measurements (Schnyder 1992). Moreover, the external precision of $^{13}\text{CO}_2/^{12}\text{CO}_2$ measurements was very high ($\text{SD} < 0.2\text{‰}$). This measure of precision included all errors associated with CO₂-free air generation, source CO₂ composition, gas mixing, sampling and determination of $^{13}\text{CO}_2/^{12}\text{CO}_2$ ratios (see Schnyder *et al.* 2003). Lastly, all $^{13}\text{CO}_2/^{12}\text{CO}_2$ exchange measurements were performed in the same isotopic environment as stand growth.

The data also demonstrate that daytime (photo)respired CO₂ was ^{13}C -depleted by a few permil relative to CO₂ net fixed, whereas CO₂ respired in darkness was enriched by several permil (Table 2). This variation was also observed in previous work at mesocosm-scale with sunflower growing at 200 and 1000 $\mu\text{mol mol}^{-1}$ CO₂ (Tcherkez *et al.* 2010) and in leaf-scale studies (Ghashghaie *et al.* 2003; Tcherkez *et al.* 2004) and is probably related (at least in part) to diurnal variations in the isotopic composition of sucrose (Gessler *et al.* 2008), the main substrate for respiratory metabolism.

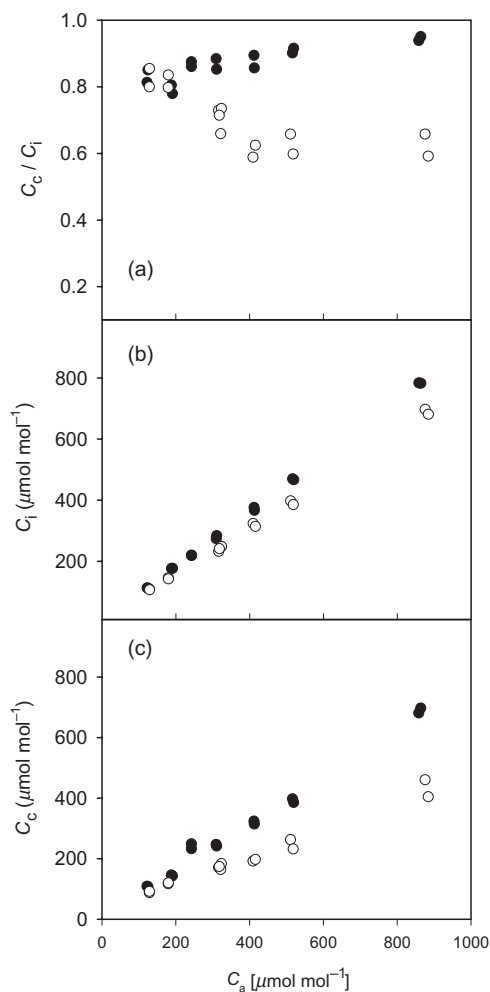


Figure 5. Ratio of C_c to C_i (a), C_i (b) and C_c (c) in ABA-treated (open symbols) and control (full symbols) sunflower canopies as a function of C_a .

These variations result from an isotope effect of aldolases (Gleixner & Schmidt 1997) that catalyse the production of fructose-1,6-bisphosphate from triose phosphates. This causes a circadian variation in the ^{13}C content of sucrose, depleting sucrose formed in light, and enriching sucrose formed from transitory starch at night (Tcherkez *et al.* 2010). Perhaps, the divergent effect ABA on δ_{PR} is also related to an ABA effect on C metabolism. Water stress can change C partitioning between starch and soluble sugars (sucrose and hexoses) synthesis in favour of sugars (Vassey & Sharkey 1989; Kanechi *et al.* 1998), to assist osmotic adjustment (Villadsen, Rung & Nielsen 2005). External addition of ABA can also cause changes in the activity of enzymes associated with primary carbohydrate metabolism (Yang *et al.* 2004). In this context, it is interesting to note that after ABA application, the (photo)respiratory flux was slightly ^{13}C -enriched relative to that net fixed (Table 2). This effect could be related to an inhibition of starch biosynthesis by ABA, which would lead to less negative $\delta^{13}\text{C}$ of triose phosphates exported from chloroplasts during the light period. This effect would also cause a less negative $\delta^{13}\text{C}$ of sucrose synthesized in the cytoplasm and exported to other plant parts.

The g_{m} responses observed here were highly dynamic and fully reversible, and were unrelated to anatomical features. This corroborates the view that g_{m} has a protein- or enzyme-facilitated component (Bernacchi *et al.* 2002; Warren & Dreyer 2006; Flexas *et al.* 2007) with aquaporins as likely candidates. In tobacco leaves, the highest concentration was found in cells adjoining to the substomatal cavities (Otto & Kaldenhoff 2000). Aquaporins can mediate CO_2 transport across membranes (Maurel *et al.* 2008), and in tobacco were shown to enhance membrane permeability for CO_2 (Uehlein *et al.* 2003). Overexpression in rice (Hanba *et al.* 2004) and tobacco (Flexas *et al.* 2006) significantly increased g_{m} . Flexas *et al.* (2007) hypothesized that maintaining high g_{m} could be an energy consuming process. Thus, at low C_{a} , when CO_2 availability is limiting photosynthesis, the excess energy could be used to increase g_{m} . At high C_{a} , diverting energy to maintain a high g_{m} would be less efficient, as the extra CO_2 at the site of carboxylation would result in only little additional CO_2 fixation. In our study, the modulation of g_{m} seemed strictly dependent on the presence of ABA. The mechanism underlying this effect is presently unclear. However, if aquaporins played a role, then it should be interesting to investigate ABA effects on their CO_2 transport function. Interestingly, the CO_2 response of g_{m} observed at the mesocosm scale, and the effect of ABA on this response, differed from that observed at leaf-scale by Vrabl *et al.* (2009). In the presence of ABA, they found a similar CO_2 response of g_{m} in the reliable range of their data. However, in controls, they also observed a decrease of g_{m} with increasing CO_2 , while we found no effect. Absence of a CO_2 effect on g_{m} has also been observed by others (see compilation in Flexas *et al.* 2008). It is well possible, that the difference between the leaf- (Vrabl *et al.* 2009) and the present mesocosm-scale CO_2 response of g_{m} was related to interactions with other external factors, such as light and

CO_2 exposure of plants. The leaf measurements of Vrabl *et al.* occurred in high light (irradiance was >2 times higher than during growth), whereas our measurements were performed at the same irradiance as during growth ($600 \mu\text{mol m}^{-2} \text{s}^{-1}$ PPFD). Interestingly, Flexas *et al.* (2007) showed that in tobacco the response of g_{m} to a change in CO_2 concentration was far less pronounced at low compared with high light intensity during measurements. Furthermore, Vrabl *et al.* (2009) measured the CO_2 response on a portion of a leaf, whereas the remaining part and all other leaves experienced a different CO_2 concentration. This contrasts with the mesocosm-scale response, which was obtained by exposing all leaves to the same CO_2 . Lastly, Vrabl *et al.* (2009) measured only young leaves, whereas all leaf-age categories of plants contributed to the mesocosm-scale measurement. It is known that physiological responses to ABA addition can depend on interactions with particular environmental scenarios (Tardieu, Parent & Simonneau 2010), and availability of light could be an important factor.

ACKNOWLEDGMENTS

Guillaume Tcherkez is thanked for helpful discussions and Thomas Gebbing and Wolfgang Feneis for fine help with running and maintaining the mesocosm facility. This research was partially supported by DFG (SCHN 557/4-1) and the European Community's Human Potential Program under contract HPRN-CT-1999-00059, NETCARB, coordinated by Jaleh Ghashghaie. J.S. was supported by GA CR grant 206/08-0787 and MEYS grants 6007665801 and AV0Z50510513.

REFERENCES

- Aphalo P.J. & Jarvis P.G. (1993) The boundary layer and the apparent responses of stomatal conductance to wind speed and to the mole fractions of CO_2 and water vapour in the air. *Plant, Cell & Environment* **16**, 771–783.
- Bernacchi C.J., Portis A.R., Nakano H., von Caemmerer S. & Long S.P. (2002) Temperature response of mesophyll conductance. Implications for the determination of Rubisco enzyme kinetics and for limitations to photosynthesis in vivo. *Plant Physiology* **30**, 1992–1998.
- von Caemmerer S. & Evans J.R. (1991) Determination of the average partial pressure of CO_2 in chloroplasts from leaves of several C_3 plants. *Australian Journal of Plant Physiology* **18**, 287–305.
- von Caemmerer S. & Farquhar G.D. (1981) Some relationships between the biochemistry of photosynthesis and the gas exchange of leaves. *Planta* **153**, 367–387.
- Connor D.J., Sadras V.O. & Hall A.J. (1995) Canopy nitrogen distribution and the photosynthetic performance of Sunflower crops during grain filling – a quantitative analysis. *Oecologia* **101**, 274–281.
- Craig H. (1954) Carbon 13 in plants and the relationship between Carbon 13 and Carbon 14 variations in nature. *Journal of Geology* **62**, 115–149.
- Epron D., Godard D., Cornic G. & Genty B. (1995) Limitation of net CO_2 assimilation rate by internal resistances to CO_2 transfer in the leaves of 2 tree species (*Fagus sylvatica* L. and *Castanea sativa* Mill.). *Plant, Cell & Environment* **18**, 43–51.

- Evans J.R. & von Caemmerer S. (1996) Carbon dioxide diffusion inside leaves. *Plant Physiology* **110**, 339–346.
- Evans J.R., Sharkey T.D., Berry J.A. & Farquhar G.D. (1986) Carbon isotope discrimination measured concurrently with gas exchange to investigate CO₂ diffusion in leaves of higher plants. *Australian Journal of Plant Physiology* **13**, 281–292.
- Evans J.R., Kaldenhoff R., Genty B. & Terashima I. (2009) Resistances along the CO₂ diffusion pathway inside leaves. *Journal of Experimental Botany* **60**, 2235–2248.
- Farquhar G.D. (1983) On the nature of carbon isotope discrimination in C₄ species. *Australian Journal of Plant Physiology* **10**, 205–226.
- Farquhar G.D., von Caemmerer S. & Berry J.A. (1980) A biochemical model of photosynthetic CO₂ assimilation in leaves of C₃ species. *Planta* **149**, 78–90.
- Flexas J., Ribas-Carbo M., Hanson D.T., Bota J., Otto B., Cifre J., McDowell N., Medrano H. & Kaldenhoff R. (2006) Tobacco aquaporin NtAQP1 is involved in mesophyll conductance to CO₂ in vivo. *The Plant Journal* **48**, 427–429.
- Flexas J., Diaz-Espejo A., Galmes J., Kaldenhoff R., Medrano H. & Ribas-Carbo M. (2007) Rapid variations of mesophyll conductance in response to changes in CO₂ concentration around leaves. *Plant, Cell & Environment* **30**, 1284–1298.
- Flexas J., Ribas-Carbo M., Diaz-Espejo A., Galmes J. & Medrano H. (2008) Mesophyll conductance to CO₂: current knowledge and future prospects. *Plant, Cell & Environment* **31**, 602–621.
- Gan K.S., Wong S.C., Yong J.W.H. & Farquhar G.D. (2002) ¹⁸O Spatial patterns of vein xylem water, leaf water, and dry matter in cotton leaves. *Plant Physiology* **130**, 1008–1021.
- Gessler A., Tcherkez G., Peuke A.D., Ghashghaie J. & Farquhar G.D. (2008) Experimental evidence for diel variations of the carbon isotope composition in leaf, stem and phloem sap organic matter in *Ricinus communis*. *Plant, Cell & Environment* **31**, 941–953.
- Ghashghaie J., Badeck F., Lanigan G., Nogués S., Tcherkez G., Delèens E., Cornic G. & Griffiths H. (2003) Carbon isotope fractionation during dark respiration and photorespiration in C₃ plants. *Phytochemistry Reviews* **2**, 145–161.
- Gleixner G. & Schmidt H.L. (1997) Carbon isotope effects on the fructose-1,6-bisphosphate aldolase reaction, origin for non-statistical ¹³C distributions in carbohydrates. *Journal of Biological Chemistry* **272**, 5382–5387.
- Hanba Y.T., Shibasaki M., Hayashi Y., Hayakawa T., Kasamo K., Terashima I. & Katsuhara M. (2004) Overexpression of the barley aquaporin HvPIP2;1 increases internal CO₂ conductance and CO₂ assimilation in the leaves of transgenic rice plants. *Plant and Cell Physiology* **45**, 521–529.
- Hassiotou F., Ludwig M., Renton M., Veneklaas E.J. & Evans J.R. (2009) Influence of leaf dry mass per area, CO₂, and irradiance on mesophyll conductance in sclerophylls. *Journal of Experimental Botany* **60**, 2303–2314.
- Kanechi M., Yamada J., Inagaki M. & Maekawa S. (1998) Non-stomatal inhibition of photosynthesis associated with partitioning of the recent assimilates into starch and sucrose in sunflower leaves under water stress. *Journal of the Japanese Society for Horticultural Science* **67**, 190–197.
- Klumpp K., Schäufele R., Lötscher M., Lattanzi F.A., Feneis W. & Schnyder H. (2005) C-isotope composition of CO₂ respired by shoots and roots: fractionation during dark respiration? *Plant, Cell & Environment* **28**, 241–250.
- Lloyd J., Syvertsen S.P., Kriedemann P.E. & Farquhar G.D. (1992) Low conductance for CO₂ diffusion from stomata to the sites of carboxylation in leaves of woody species. *Plant, Cell & Environment* **15**, 873–899.
- McNevin D.B., Badger M.R., Kane H.J. & Farquhar G.D. (2006) Measurement of (carbon) kinetic isotope effect by Rayleigh fractionation using membrane inlet mass spectrometry for CO₂-consuming reactions. *Functional Plant Biology* **33**, 1115–1128.
- Maurel C., Verdoucq L., Luu D.-T. & Santoni V. (2008) Plant aquaporins: membrane channels with multiple integrated functions. *Annual Review of Plant Biology* **59**, 595–624.
- Morrison J.I.L. & Gifford R.M. (1984) Plant growth and water use with limited water supply in high CO₂ concentrations. I. Leaf area, water use and transpiration. *Australian Journal of Plant Physiology* **11**, 361–374.
- Niinemets Ü., Cescatti A., Rodeghiero M. & Tosens T. (2005) Leaf internal diffusion conductance limits photosynthesis more strongly in older leaves of Mediterranean evergreen broad-leaved species. *Plant, Cell & Environment* **28**, 1552–1566.
- O'Leary M. (1984) Measurement of the isotope fractionation associated with diffusion of carbon dioxide in aqueous solution. *Journal of Physical Chemistry* **88**, 823–825.
- Otto B. & Kaldenhoff R. (2000) Cell-specific expression of the mercury-insensitive plasma-membrane aquaporin NtAQP1 from *Nicotiana tabacum*. *Planta* **211**, 167–172.
- Piel C., Frak E., Le Roux X. & Genty B. (2002) Effect of local irradiance on CO₂ transfer conductance of mesophyll in walnut. *Journal of Experimental Botany* **53**, 2423–2430.
- Schnyder H. (1992) Long-term steady-state labeling of wheat plants by use of natural ¹³CO₂/¹²CO₂ mixtures in an open, rapidly turned-over system. *Planta* **187**, 128–135.
- Schnyder H., Schäufele R., Lötscher M. & Gebbing T. (2003) Disentangling CO₂ fluxes: direct measurements of mesocosm-scale natural abundance ¹³CO₂/¹²CO₂ gas exchange, ¹³C discrimination, and labelling of CO₂ exchange flux components in controlled environments. *Plant, Cell & Environment* **26**, 1863–1874.
- Tardieu F., Parent B. & Simonneau T. (2010) Control of leaf growth by abscisic acid: hydraulic or non-hydraulic processes? *Plant, Cell & Environment* **33**, 636–647.
- Tazoe Y., von Caemmerer S., Badger M.R. & Evans J.R. (2009) Light and CO₂ do not affect the mesophyll conductance to CO₂ diffusion in wheat leaves. *Journal of Experimental Botany* **60**, 2291–2301.
- Tcherkez G., Farquhar G.D., Badeck F. & Ghashghaie J. (2004) Theoretical considerations about carbon isotope distribution in glucose of C₃ plants. *Functional Plant Biology* **31**, 857–877.
- Tcherkez G., Schäufele R., Nogués S., *et al.* (2010) On the ¹³C/¹²C isotopic signal of day and night respiration at the mesocosm level. *Plant, Cell & Environment* **33**, 900–913.
- Terashima I., Hanba Y.T., Tazoe Y., Vyas P. & Satoshi Y. (2006) Irradiance and phenotype: comparative eco-development of sun and shade leaves in relation to photosynthetic CO₂ diffusion. *Journal of Experimental Botany* **57**, 343–354.
- Uehlein N., Lovisolo C., Siefritz F. & Kaldenhoff R. (2003) The tobacco aquaporin NtAQP1 is a membrane CO₂ pore with physiological functions. *Nature* **425**, 734–737.
- Vassey T.L. & Sharkey T.D. (1989) Mild water stress of *Phaseolus vulgaris* plants leads to reduced starch synthesis and extractable sucrose phosphate synthase activity. *Plant Physiology* **89**, 1066–1070.
- Villadsen D., Rung J.H. & Nielsen T.H. (2005) Osmotic stress changes carbohydrate partitioning and fructose-2,6-bisphosphate metabolism in barley leaves. *Functional Plant Biology* **32**, 1033–1043.
- Vogel J.C., Grootes P.M. & Mook W.G. (1970) Isotopic fractionation between gaseous and dissolved carbon dioxide. *Zeitschrift für Physik A Hadrons and Nuclei* **230**, 225–238.

- Vrabl D., Vaskova M., Hronkova M., Flexas J. & Santrucek J. (2009) Mesophyll conductance to CO₂ transport estimated by two independent methods: effect of variable CO₂ concentration and abscisic acid. *Journal of Experimental Botany* **60**, 2315–2323.
- Warren C. (2006) Estimating the internal conductance to CO₂ movement. *Functional Plant Biology* **33**, 431–442.
- Warren C.R. & Dreyer E. (2006) Temperature response of photosynthesis and internal conductance to CO₂: results from two independent approaches. *Journal of Experimental Botany* **57**, 3057–3067.
- Yang J.C., Zhang J.H., Wang Z.Q., Zhu Q.S. & Liu L.J. (2004) Activities of fructan- and sucrose-metabolizing enzymes in wheat stems subjected to water stress during grain filling. *Planta* **220**, 331–343.

Received 9 June 2010; received in revised form 27 August 2010; accepted for publication 30 August 2010

SUPPORTING INFORMATION

Additional Supporting Information may be found in the online version of this article:

Figure S1. Water-use efficiency (WUE) in ABA-treated (open symbols) and control (full symbols) sunflower canopies as a function of C_a . WUE was calculated as the ratio of A to E . Lines are fitted for ease of comparison.

Please note: Wiley-Blackwell are not responsible for the content or functionality of any supporting materials supplied by the authors. Any queries (other than missing material) should be directed to the corresponding author for the article.